PCCP

Accepted Manuscript

ARTICLE TYPE

Magnetic anomalies and itinerant character of electrochemically Li-inserted Li[Li$_{1/3}$Ti$_{5/3}$]O$_4$†

Kazuhiko Mukai,^{*a} **Jun Sugiyama**^{a}

Spinel oxides of Li[Li$_y$Ti$_{2-y}$]O$_4$ with $0 \leq y \leq 1/3$ exhibit two glamorous features for solid state chemistry and condensed matter physics. The one is a reversible lithium insertion/extraction reaction, in particular for Li[Li$_{1/3}$Ti$_{5/3}$]O$_4$, and the other is a superconducting transition at $T_c \simeq 13$ K for Li[Ti$_2$]O$_4$. To study the change in magnetic environments of the $y = 1/3$ compound with excess Li (x), we measured magnetic susceptibility (χ) for the Li$_{1+x}$[Li$_{1/3}$Ti$_{5/3}$]O$_4$ samples with $0 \leq x \leq 0.95$, which were prepared by an electrochemical Li insertion reaction into Li[Li$_{1/3}$Ti$_{5/3}$]O$_4$. Even for the $x = 0$ sample, two magnetic anomalies were found at T_{m1}^{on} (= 63 K) and T_{m2}^{on} (= 21 K), despite the fact that all Ti ions should be in the 4+ state with $S = 0$. A comparative study of TiO$_2$ and Li$_2$TiO$_3$ revealed that these magnetic anomalies are not impurity-induced effects but are caused by an intrinsic nature of Li[Li$_{1/3}$Ti$_{5/3}$]O$_4$, probably due to either slight compositional deviation from stoichiometry or dislocations such as a Magnéli phase. For the $x > 0$ samples, the χ vs. temperature curve was found to consist of a temperature-independent Pauli-paramagnetic contribution and a Curie-Weiss contribution. Detailed analyses of χ clarified the systematic variations of the effective magnetic moment of Ti ions, effective mass of electrons in the conduction band, and density of states at the Fermi level with x, indicating that the Li$^+$ ions at the 16d site play a significant role in localizing d electrons of Ti^{3+} ions.

1 Introduction

A lithium-titanium-oxide spinel, Li[Li$_{1/3}$Ti$_{5/3}$]O$_4$ (LTO), has been widely studied as an electrode material for lithium-ion batteries (LIBs).[1,2] In the LTO spinel lattice with a cubic symmetry of space group $Fd\bar{3}m$, Li$^+$ ions occupy both tetrahedral 8a and octahedral 16d sites, Ti^{4+} ions occupy the octahedral 16d site, and O^{2-} ions occupy tetrahedral 32e site. An electrochemical Li$^+$ insertion/extraction reaction of LTO is represented by[1,2]

$$\text{Li[Li}_{1/3}\text{Ti}_{5/3}\text{]O}_4 + x\text{Li}^+ + xe^- \leftrightarrow \text{Li}_{1+x}\text{[Li}_{1/3}\text{Ti}_{5/3}\text{]O}_4, \quad (1)$$
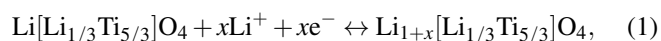
where x Li$^+$ ions are inserted into an initially vacant 16c site. During this reaction, the lattice parameter ($a_c \approx 8.35$ Å for LTO) is nearly independent of x, leading to LTO as an ideal electrode material for long cycle-life LIB.[2]

Before the discovery of the reversible Li insertion/extraction reaction, LTO and its derivatives, Li[Li$_y$Ti$_{2-y}$]O$_4$ with $0 \leq y \leq 1/3$, was mainly studied

by condensed matter physicists. This is because LiTi$_2$O$_4$ was found to enter a superconducting phase below $T_c \simeq 13$ K,[3,4] which is the highest T_c among superconducting materials with a spinel structure, such as CuRh$_2$S$_4$ (T_c = 4.5 K) and CuRh$_2$Se$_4$ (T_c = 3.5 K).[5] Since Ti ions in LTO are in the 4+ state with $S = 0$, LTO is naturally an insulator. This means that as y increases from 0, Li[Li$_y$Ti$_{2-y}$]O$_4$ shows an metal-to-insulator (MIT) transition at $y \simeq 0.11$.[4,6] This MIT transition and the superconducting transition for the $y \simeq 0$ phase have been investigated by several techniques, such as magnetic susceptibility (χ) measurements on powder[4,6] and single-crystal[7,8] samples, specific heat analyses combined with electrical resistivity measurements,[9–12] NMR spectroscopy,[13] and others.[14–16] As a result, LiTi$_2$O$_4$ is considered as a typical BCS type-II superconductor with moderate coupling and s-wave symmetry.[11,12]

More precisely, as y increases from 0, T_c is almost independent until $y = 0.11$, whereas the superconducting volume fraction (V_{sc}) decreases linearly with y, and then reaches 0 at $y \simeq 0.15$.[4,6] Fig. 1 shows the ternary phase diagram between Li$_2$TiO$_3$, TiO$_2$, and LiTiO$_2$, on which the compositions reported for the previous χ measurements[4,6] are plotted. Along the bottom edge of the triangle, TiO$_2$ is converted to LiTiO$_2$ (Li$_2$[Ti$_2$]O$_4$) via. LiTi$_2$O$_4$ by a Li-inserted reaction. In other words, the average valence of Ti ions (V_{ave}) can be reduced from +4 to +3 by a Li-inserted reaction. Indeed, Hamada et

---

al[17] prepared $Li_{1+x}Ti_2O_4$ with $x > 0$ by an electrochemical reaction and showed that V_{sc} decreases with x, while T_c is independent of x. Interestingly, even for $Li_{1+x}Ti_2O_4$ with $x < 0$, V_{sc} decreases with decreasing x, but T_c does not change with x,[17] i.e., V_{sc} reaches a maximum at $x = 1$. Such effects of y and x on T_c and V_{sc}[4,6,17] suggest that a condition of $V_{ave} = +3.5$ is important for superconductivity in the Li-Ti-O system.

The previous χ measurements of the Li-Ti-O system were performed only for $Li[Li_yTi_{2-y}]O_4$[4,6] and $Li_xTi_2O_4$.[17] which are represented by black circles and triangles in Fig. 1. To better understand the magnetic nature of the Li-Ti-O system, we need to measure χ along the other lines in the phase diagram. In particular, the line between $Li[Li_{1/3}Ti_{5/3}]O_4$ and $Li_2[Li_{1/3}Ti_{5/3}]O_4$, which corresponds to the reaction in eqn (1), is worth studying, because the spinel framework is maintained in the whole x range,[1,2] and consequently, we could understand the change in magnetism without a structural consideration on the core matrix. Furthermore, such study is important for understanding the interrelationship between low-temperature physical properties and high-temperature electrochemical properties in LIB materials. For instance, the operative voltage for LTO is 1.55 V vs. Li^+/Li,[1,2] whereas that for $LiTi_2O_4$ is 1.38 V,[1,17] despite the fact that the Ti^{4+}/Ti^{3+} ions are reduced/oxidized in the spinel lattice for both materials.

In this study, the Li-inserted LTO samples were prepared by the electrochemical reaction shown in eqn (1), because a chemical Li^+ insertion/extraction reaction is known to induce complicated structural transformations.[18,19] The composition employed for this study is shown as red circles in Fig. 1. Note that, even in the end compound, $Li_2[Li_{1/3}Ti_{5/3}]O_4$, 40 % of Ti ions are in the 4+ state, due to a limited number of vacant sites for the inserted Li^+ ion.[2] We also measured χ for the $x = 5/6$ sample, because V_{ave} of this composition is +3.5 (see dotted blue line in Fig. 1).

2 Experimental details

A powder LTO sample was synthesized by a solid-state reaction technique, as reported previously.[20,21] A stoichiometric mixture of $LiOH \cdot H_2O$ (Wako Pure Chemical Industries, Ltd., 98 %) and TiO_2 anatase (Wako Pure Chemical Industries, Ltd., > 98.5 %) was mixed with a mortar and pestle and pressed into a pellet with 23 mm diameter and ~5 mm thickness. The pellet was heated at 1023 K in air for 12 h, followed by heating at 673 K in air for 12 h. The obtained LTO powder was characterized by powder X-ray diffraction (XRD) measurements using a Cu-Kα radiation (RINT-TTR, Rigaku Co. Ltd.) and electrochemical charge/discharge tests using a conventional electrode mix. Details for preparing the electrode mix are described elsewhere.[20] Powder TiO_2 anatase, TiO_2 rutile, and Li_2TiO_3 samples were also prepared as follows. The TiO_2 anatase and TiO_2 rutile samples were prepared by
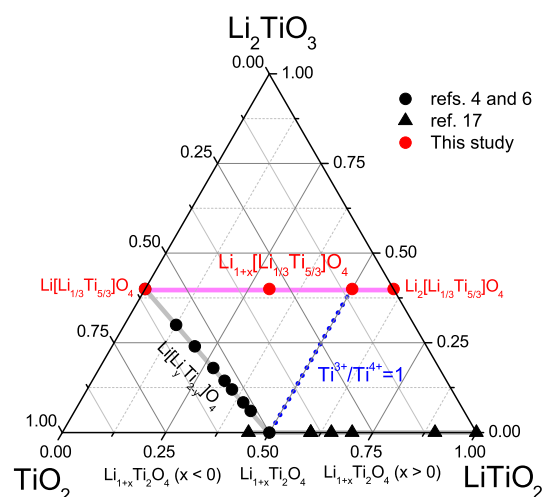
Fig. 1 Ternary phase diagram for the Li-Ti-O system in the region bounded by Li_2TiO_3, TiO_2, and $LiTiO_2$. $Li[Li_{1/3}Ti_{5/3}]O_4$ and $LiTi_2O_4$ form a solid solution compound, $Li[Li_yTi_{2-y}]O_4$, in the y range between 0 and 1/3. Closed red circles represent the Li composition (x) in $Li_{1+x}[Li_{1/3}Ti_{5/3}]O_4$ of this study, which was prepared by the electrochemical reaction described in eqn (1). Closed black circles and triangles show previous magnetic studies on $Li[Li_yTi_{2-y}]O_4$[4,6] and $Li_{1+x}Ti_2O_4$,[17] respectively. Dotted blue line indicates the composition at which the average valence of the Ti ions is +3.5.

heating the as-received TiO_2 anatase at 873 K in air for 12 h and 1173 K in air for 12 h, respectively. The Li_2TiO_3 sample was synthesized by heating a mixture of $LiOH \cdot H_2O$ and TiO_2 anatase at 1173 K in air for 12 h.

Lithium-inserted LTO samples for the χ measurements were prepared by the electrochemical reaction shown in eqn (1). Approximately 50 mg of LTO powder was pressed into a pellet with a 10 mm diameter and the pellet was used as a working electrode in nonaqueous lithium cell. A lithium metal sheet pressed on a stainless steel plate ($\phi = 19$ mm) was used as a counter electrode. The electrolyte was 1 M $LiPF_6$ dissolved in an ethylene carbonate (EC)/diethyl carbonate (DEC) (EC/DEC = 1/1 by volume ratio) solution (Kishida Chemical Co. Ltd.) The cell was slowly discharged to a desired Li composition with a constant current of 0.1 mA ($\simeq 0.127$ mA/cm^2). The Li composition was evaluated by an inductively coupled plasma-atomic emission spectroscopic (ICP-AES, CIROS 120, Rigaku Co. Ltd., Japan) analysis. The above procedure is the same as that of our previous χ measurements on Li_xNiO_2[19] and $Li_x[Ni_{1/2}Mn_{3/2}]O_4$.[22]

χ (= M/H) was obtained in both field-cooling (FC)

and zero-field-cooling (ZFC) modes using a superconducting quantum interference device (SQUID) magnetometer (MPMS, Quantum Design) under a magnetic field (H) with 10 kOe. The Li-inserted sample was removed from the lithium cell in an Ar-filled glove-box just before the χ measurements. The sample was then packed into two 20 mm × 20 mm Al foil sheets and attached to the sample rod with a Cu wire. We first measured magnetization (M) using FC mode in the T range between 5 and 300 K with H = 10 kOe. We then measured M using a combination of ZFC and FC mode with H = 10 and 100 Oe in the T range between 5 and 100 K. Only for $x = 0$, χ was measured for two commercially available Li[Li$_{1/3}$Ti$_{5/3}$]O$_4$ samples; LT-1 and LT-106 (ENERMIGHT) purchased by Titan Kogyo, Ltd. and Ishihara Sangyo Kaisha, Ltd., respectively.

3 Results

3.1 χ measurements of initial LTO and other lithium titanium oxides

A Rietveld analysis of the XRD pattern for the LTO sample indicated that the sample is a single-phase with a spinel structure (Fig. S1 of the Supplementary Information). The lattice parameter (a_c) was determined to be 8.357(1) Å, which is comparable to the previously reported a_c.[1,2,20,21] Furthermore, electrochemical charge/discharge measurements confirmed that the rechargeable capacity (Q_{recha}) of LTO is ~165 mAh/g, which is ~94 % of the theoretical capacity (Q_{theo} = 175 mAh/g), based on the reaction in eqn (1). These results mean that nearly all Ti ions in the LTO sample are in the 4+ state with $S = 0$. Despite this, the $\chi(T)$ curve shows two magnetic anomalies at around 63 K(= T_{m1}) and 21 K(= T_{m2}), as seen in Fig. 2(a). As T decreases from 300 K, χ is roughly T-independent (~10 × 10^{-6} emu·Ti-mol^{-1}) down to 80 K, then suddenly increases by ~40 × 10^{-6} emu·Ti-mol^{-1} with decreasing T, followed by a rapid increase by ~100 × 10^{-6} emu·Ti-mol^{-1} with further decreasing T. Because the contributions from the Al foils and Cu wire were subtracted from the data, these magnetic anomalies are likely to come from the LTO sample. We also performed χ measurements on the two commercial available LTOs. As shown in the Fig. S2 of the Supplementary Information, two magnetic anomalies are also observed at around 70 and 20 K, although their absolute χ values differ each other especially below 70 K.

To determine the effect of impurities in the LTO sample, which may contain Fe and/or Mn oxides in the as-received TiO$_2$ anatase powder (98.5% purity), we measured χ for other lithium titanium oxides. Figs. 2(b) and 2(c) show the T dependence of χ for the TiO$_2$ anatase, TiO$_2$ rutile, and Li$_2$TiO$_3$ samples. For TiO$_2$ anatase, magnetic anomalies are also ob-

served at around 70 and 20 K, whereas no magnetic anomaly is seen as low as 5 K for TiO$_2$ rutile. Namely, χ is almost constant at ~30 × 10^{-6} emu·Ti-mol^{-1} in the T range between 5 and 300 K. For Li$_2$TiO$_3$, another magnetic anomaly around 130 K as well as two anomalies around 60 and 20 K were observed. Here, both TiO$_2$ rutile and Li$_2$TiO$_3$ were prepared from the same TiO$_2$ anatase powder by a solid state reaction technique at T = 1173 K. If impurities in the TiO$_2$ anatase induce the magnetic anomalies at 70 and 20 K, such anomalies should also be expected in TiO$_2$ rutile. Therefore, the absence of magnetic anomalies in TiO$_2$ rutile suggests that the two magnetic anomalies in LTO are an intrinsic feature of the LTO sample.
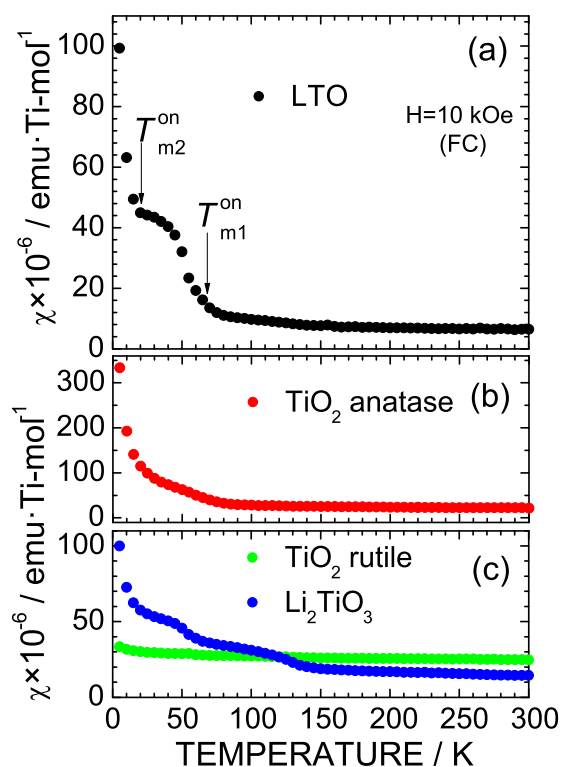
Fig. 2 (a) Temperature dependence of magnetic susceptibility (χ) for the (a) Li[Li$_{1/3}$Ti$_{5/3}$]O$_4$ (LTO) sample. χ was measured in a field-cooling (FC) mode with H = 10 kOe. T_{m1}^{on} (= 63 K) and T_{m2}^{on} (= 21 K) are the onsets of the magnetic transition temperatures for the LTO sample. χ for TiO$_2$ anatase is shown in (b), while those for TiO$_2$ rutile and Li$_2$TiO$_3$ are shown in (c).

3.2 Preparation of Li-inserted LTO samples

Fig. 3 shows the discharge curve of the Li/LTO cell for the present χ measurements. The discharge curve of one cell is

identical to those of the other cells, i.e., at a very early stage of the Li insertion reaction ($x \leq 0.01$), the operating voltage rapidly drops to ~1.6 V with x, then levels off to an nearly constant value (1.55 V) until $x \simeq 0.9$, and finally rapidly drops again to ~1.0 V with further increasing x. Because the discharge curve for the Li/LTO cell with a mixed electrode, which consists of LTO, conducting carbon, and binder, is equivalent to those for the Li/LTO cell with an LTO electrode, the electrochemical reaction for the LTO electrode is found to proceed homogeneously. The values of x in $Li_{1+x}[Li_{1/3}Ti_{5/3}]O_4$ for the three samples were estimated as 0.50, 0.83, and 0.95 from the ratio between the discharged capacity and Q_{theo}. As seen in the inset of Fig. 3, these x values are in good agreement with those determined by ICP-AES analyses. Hereafter, we use the x value determined by the discharge capacity. Notably, the chemical formula for the $x = 0.83$ sample is close to $Li_{11/6}[Li_{1/3}Ti_{5/6}^{3+}Ti_{5/6}^{4+}]O_4$. If we ignore the contributions of the inserted Li ions at the $16c$ site, we can understand the effects of the Li ions at the $16d$ site on magnetism by comparing the result of $LiTi_2O_4$ ($Li[Ti^{3+}Ti^{4+}]O_4$).

x in $Li_{1+x}[Li_{1/3}Ti_{5/3}]O_4$

x	
EC*	ICP-AES
0	0.02
0.50	0.51
0.83	0.83
0.95	1.00

*Electrochemical reaction
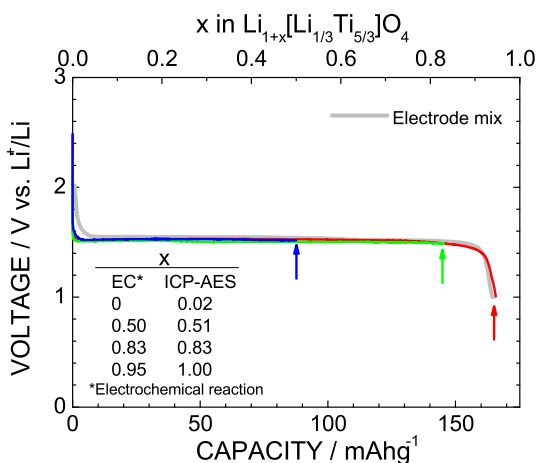
Fig. 3 Discharge curves of the $Li/Li[Li_{1/3}Ti_{5/3}O_4$ (LTO) cells for the χ measurements. The cells were slowly discharged at a current density of 0.127 mA/cm^2, because the electrode contained no conducting carbon and binder. Each arrow indicates the Li composition for the χ measurements. The x values in $Li_{1+x}[Li_{1/3}Ti_{5/3}]O_4$ were determined by both discharge capacity and ICP-AES analysis (see inset). The discharge curve of the Li/LTO cell, in which both conducting carbon and binder were used as an electrode (electrode mix), was also shown to clarify the homogeneous electrochemical reaction.

3.3 χ measurements of Li-inserted LTO

Fig. 4(a) shows the T dependence of χ for the $Li_{1+x}[Li_{1/3}Ti_{5/3}]O_4$ samples with $x = 0$, 0.50, 0.83, and 0.95. The T dependence of inverse χ for the four samples is shown in Figs. 4(b) and 4(c). For the $x = 0.50$ sample, as T decreases from 300 K, χ gradually increases with decreasing T down to ~60 K, followed by an increase with a slight different slope ($d\chi/dT$) below 60 K. Such behavior can be seen more clearly in the $\chi^{-1}(T)$ curve. The magnitude of χ at 5 K is ~1.8×10^{-3} emu·Ti-mol^{-1}, which is about twenty times larger than χ at 5 K for the $x = 0$ sample. The increase in χ below 60 K, in other words, a Curie-Weiss behavior, indicates the presence of localized moments caused by the formation of Ti^{3+} ions with $S = 1/2$ (d^1) due to the Li insertion into the LTO lattice. As x increases from 0.50 to 0.95 via 0.83, not only a Curie-Weiss behavior but also a T-independent χ, i.e., χ at high T, are enhanced with x. This suggests the increase in both the effective magnetic moment of Ti ion and density of states at the Fermi level with x, as discussed later.

To clarify the existence or absence of magnetic transitions at low-T, Fig. 5 shows the T dependence of χ for the $Li_{1+x}[Li_{1/3}Ti_{5/3}]O_4$ samples with $x = 0$, 0.50, 0.83, and 0.95 measured in both ZFC and FC modes with $H = 100$ Oe. For the $x = 0$ sample, the $\chi(T)$ curve obtained in the FC mode [$\chi_{FC}(T)$] deviates from that obtained in the ZFC mode [$\chi_{ZFC}(T)$] below around 54 K. This suggests the presence of a ferromagnetic, ferrimagnetic, or spin-glass freezing transition at T_{m1}. To eliminate the effects of T_{m1}, we performed χ measurements in both ZFC and FC modes below 30 K. As shown in Fig. S3 of the Supplementary Information, the $\chi_{FC}(T)$ curve almost traces the $\chi_{ZFC}(T)$ curve even with $H = 100$ Oe, indicating a paramagnetic (PM) behavior below 30 K.

For the samples with $x \geq 0.50$, a similar difference between the $\chi_{FC}(T)$ and $\chi_{ZFC}(T)$ curve is observed below around 54 K ($= T_{m1}$). This confirms that the magnetic transition at T_{m1} is an intrinsic nature of the present samples, as already mentioned. To know superconductivity in the Li-inserted phase, χ was measured with $H = 10$ Oe, which is thought to be well below H_{c1}, for the $x = 0.83$ and 0.95 samples. Here H_{c1} is the lower critical field defined at the point of departure from linear dependence of $M(H)$ and is reported as ~200 Oe for $LiTi_2O_4$ [10,11]. For both samples, the $\chi_{FC}(T)$ curve was almost identical to the $\chi_{ZFC}(T)$ curve down to 5 K (Fig. S4 of the Supplementary Information). This demonstrates the absence of superconductivity above 5 K for the samples with $x = 0.83$ and 0.95, whereas $T_c \simeq 13$ K for $LiTi_2O_4$ [3,4].

4   Discussion

4.1   Origins for T_{m1} and T_{m2}

In the ideal LTO ($= Li[Li_{1/3}Ti_{5/3}]O_4$), all the Ti ions should be in the 4+ state with $S = 0$ (d^0). However, the two mag-
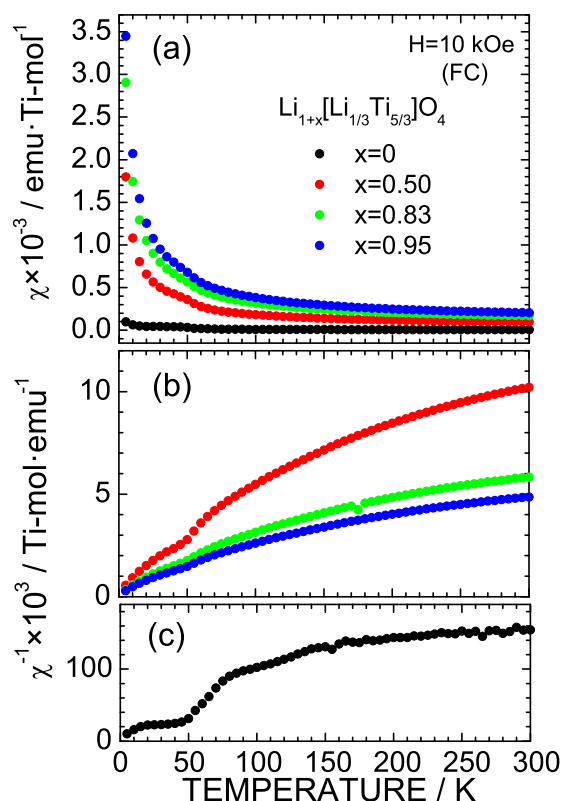
Fig. 4 Temperature dependence of magnetic susceptibility (χ) for the $Li_{1+x}[Li_{1/3}Ti_{5/3}]O_4$ samples with $x = 0$, 0.50, 0.83, and 0.95. χ was measured in a field-cooling mode with $H = 10$ kOe. Inverse χ (χ^{-1}) was shown in (b) for the $x = 0.50$, 0.83, and 0.95 samples, and (c) for the $x = 0$ sample.

Fig. 5 Temperature dependence of magnetic susceptibility (χ) for the $Li_{1+x}[Li_{1/3}Ti_{5/3}]O_4$ samples with $x = 0$, 0.50, 0.83, and 0.95. χ was measured in both zero-field-cooling (ZFC) and field-cooling (FC) modes with $H = 100$ Oe. Open and closed circles indicate χ in the FC and χ in the ZFC modes, respectively.

netic anomalies of T_{m1} and T_{m2} were observed for both synthesized and purchased LTO samples [Figs. 2(a) and S2]. To the best of our knowledge, there are no reports on such magnetism in LTO, because LTO is believed to be a nonmagnetic insulator. To explain the origin of the two magnetic anomalies, we need to assume the presence of Ti^{3+} ions with a d^1 ($S = 1/2$) state. There are two possible scenarios for the formation of Ti^{3+} in $Li[Li_{1/3}Ti_{5/3}]O_4$. One is the presence of excess cations in the lattice, and the other is the lack of oxygen anions. In fact, when LTO is heated in H_2 atmosphere, H^+ ions are inserted into the lattice.[14] However, since the present LTO was prepared in air, it is highly unlikely that H^+ ions are introduced into the LTO lattice. Conversely, if Li^+ ions are replaced by Ti ions during the preparation of LTO at high-T, i.e., a $Li[Li_{(1-\delta)/3}Ti_{(5+\delta)/3}]O_4$ phase is more stable than the stoichiometric LTO under the present preparation condition, the Ti^{3+} ions with the content $\delta/3$ are formed in

the lattice. Therefore, the origins for T_{m1} and T_{m2} are most likely due to either a slight compositional deviation from stoichiometry or dislocations like a Magnéli phase with Ti_nO_{2n-1} ($4 \leq n \leq 9$).[23,24] On the contrary for T_{m2}, since the $\chi_{FC}(T)$ curve almost traced the $\chi_{ZFC}(T)$ curve below 30 K, impurities such as Fe and/or Mn oxides would also contribute its evolution. However, since the XRD data revealed that the LTO sample is a single-phase of the spinel LTO, δ is considered to be very small. This leads to the possibility that the previous LTO compounds were not $Li[Li_{1/3}Ti_{5/3}]O_4$, but $Li[Li_{(1-\delta)/3}Ti_{(5+\delta)/3}]O_4$.

The $\chi(T)$ curves for both LTO and the raw material, TiO_2 anatase, imply the common origin for the two magnetic anomalies [Figs. 2(a) and 2(b)]. However, the two magnetic anomalies disappear for the TiO_2 rutile sample [Fig. 2(c)], which is made from the TiO_2 anatase by heating at 1173 K in air. This supports the presence of the Ti^{3+} ions with $S = 1/2$, i.e., the Li deficient phase in the raw material, TiO_2 anatase. Considering the $\chi(T)$ curve for Li_2TiO_3, such Li deficient phase is stabilized both in LTO and Li_2TiO_3 by a slight decrease in the Li content from the stoichiometric.

As seen in Fig. 5, magnetic transition at T_{m1} was also observed for the Li-inserted samples, indicating that the region of the Li deficient phase does not participate in the electrochemical reaction. Unfortunately, based only on structural, electrochemical, and magnetization measurements, there is no information on distribution of the Li deficient phase in the LTO sample. However, recent our muon-spin rotation and relaxation and ^8Li β-NMR measurements on LTO suggest that lo-

calized moments appear in the whole volume of the sample at low-T, indicating that δ distributes in the whole LTO particle. Although Q_{recha} for the present LTO reaches $\sim$94 % of Q_{theo} (Fig. 3), annihilation of the Li deficient phase would provide a larger Q_{recha} that is close to Q_{theo}. In other words, χ measurements is an effective method to know a quality of an LTO sample.
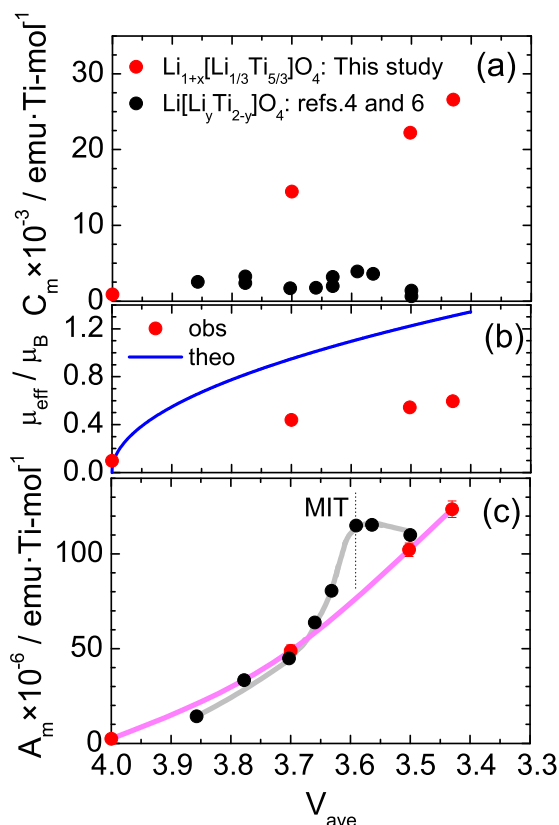
Fig. 6 Variations of (a) Curie-Weiss term (C_m), (b) effective magnetic moment (μ_{eff}), and temperature-independent term (A_m) as a function of the average valence of Ti ions (V_{ave}) in Li$_{1+x}$[Li$_{1/3}$Ti$_{5/3}$]O$_4$. C_m and A_m were determined by fitting the $\chi(T)$ curve with eqn (2). C_m and A_m for Li[Li$_y$Ti$_{2-y}$]O$_4$ obtained from refs. 4 and 6 were also illustrated in (a) and (c), respectively, for comparison. Theoretical μ_{eff} (μ_{eff}^{theo}) was calculated under the assumption that all the Ti^{3+} ions are in a magnetic $S = 1/2$ (d^1) state and that gyromagnetic factor is 2. MIT is the metal-to-insulator transition at $y \simeq 0.11$ in Li[Li$_y$Ti$_{2-y}$]O$_4$.

4.2 Comparison of Li$_{1+x}$[Li$_{1/3}$Ti$_{5/3}$]O$_4$ and Li[Li$_y$Ti$_{2-y}$]O$_4$

As indicated above, there are two main contributions in the $\chi(T)$ curves for the $x > 0$ samples. One is a Curie-Weiss contribution and the other is a Pauli PM contribution. According to the previous work on Li[Li$_y$Ti$_{2-y}$]O$_4$,[4,6] the $\chi(T)$ curve was fitted by

$$\chi = C_m/(T + \theta) + f_m(T), \qquad (2)$$

where C_m is the Cuire-Weiss term, θ is the Weiss temperature, and $f(T)$ [$= A_m + B_m(T)$] is the weakly T-dependent term which comes from both Pauli PM and Landau diamagnetic contributions. C_m is also represented by

$$C_m = \frac{N\mu_{eff}^2}{3k_B}, \qquad (3)$$

where N is the number density of Ti ions, μ_{eff} is the effective magnetic moment of Ti ions, and k_B is the Boltzmann's constant. We first attempted to fit the $\chi(T)$ curve with eqn (2) and found that the reduced χ^2, which is an indicator of fitting reliability, is not affected by the presence of the $f_m(T)$ term. Finally, the $\chi(T)$ curve was fitted with eqn (2) with $B_m = 0$, in the T range between 5 and 300 K. Only for the $x = 0$ sample, the $\chi(T)$ curve was fitted in the T range between 60 and 300 K in order to eliminate the effect of the magnetism below T_{m1}.

Fig. 6 shows the V_{ave} dependence of (a) C_m, (b) μ_{eff}, and (c) A_m for Li$_{1+x}$[Li$_{1/3}$Ti$_{5/3}$]O$_4$ together with the data for Li[Li$_y$Ti$_{2-y}$]O$_4$[4,6] for comparison. Numerical data are listed in Table 1. As V_{ave} decreases from 4+, C_m for Li$_{1+x}$[Li$_{1/3}$Ti$_{5/3}$]O$_4$ is found to increase almost linearly with decreasing V_{ave} down to about +3.4. This behavior is very different from that for Li[Li$_y$Ti$_{2-y}$]O$_4$, for which $C_m \simeq 3 \times 10^{-6}$ emu·Ti-mol^{-1} and lacks a dependence on V_{ave}, indicating an itinerant electron nature. The difference in C_m between Li$_{1+x}$[Li$_{1/3}$Ti$_{5/3}$]O$_4$ and Li[Li$_y$Ti$_{2-y}$]O$_4$ suggests that the Li ions at the 16d site play a significant role in localizing d electrons of the Ti^{3+} ions.

Assuming that the gyromagnetic (g) factor is 2 for Ti ions, μ_{eff} for each sample was estimated with eqn (3). As seen in Fig. 6(b), μ_{eff} monotonically increases with decreasing V_{ave}, as in the case for C_m. Note that even for the $x = 0.95$ sample, μ_{eff} is only $\sim$36 % of the full μ_{eff} value (μ_{eff}^{theo}) for the Ti^{3+} ion with $S = 1/2$ (d^1). Here μ_{eff}^{theo} is calculated by

$$\mu_{eff}^{theo} = g \times \sqrt{S(S+1) \times x}, \qquad (4)$$

where $x = (20 - 5V_{ave})/3$. Since $(5/3 - x)$ of Ti^{4+} ions still exists in the Li-inserted LTO, $\sim$36 % of μ_{eff}^{theo} shows that $\sim$57 % of d electrons are localized in the $x = 0.95$ sample.

Table 1 Physical parameters determined by magnetic susceptibility measurements on the $Li_{1+x}[Li_{1/3}Ti_{5/3}]O_4$ samples with $x = 0$, 0.50, 0.83, and 0.95.

x in $Li_{1+x}[Li_{1/3}Ti_{5/3}]O_4$	C_m ($10^{-6} \times$ emu·Ti-mol^{-1})	A_m ($10^{-3} \times$ emu·Ti-mol^{-1})	θ (K)	m^*/m_0 –	$N_0(E_F)$ (states/eV-atom)
0	0.89(3)	2.4(3)	−4.2(4)	–	–
0.50	14.4(3)	4.8(3)	−3.4(2)	4.5	0.37
0.83	22.2(3)	102(4)	−3.0(1)	7.9	0.76
0.95	26.6(4)	124(4)	−3.0(2)	9.1	0.91
$LiTi_2O_4$[4,6]	1.39	110	−0.9	9.4	0.97

Consequently, d electrons of the Ti^{3+} ions are not fully localized but become itinerant, indicating the evolution of a metallic behavior with decreasing V_{ave}. In fact, the T-independent term, i.e., A_m, which is an indicator for the density of states at the Fermi level, increases monotonically with decreasing V_{ave} [see Fig. 6(c)]. Furthermore, the A_m-vs.-V_{ave} curve for $Li_{1+x}[Li_{1/3}Ti_{5/3}]O_4$ is very close to that for $Li[Li_yTi_{2-y}]O_4$ at $V_{ave} < 3.6$. This suggests that the change in the electronic structure of the former system is explained by the same phenomenology to that for the latter system. It should be noted that the Li/Ti ratio at the 16d site does not change with x in the former system, while that varies with y in the latter system. At $V_{ave} \geq 3.6$, the trend in A_m for $Li_{1+x}[Li_{1/3}Ti_{5/3}]O_4$ is different from that for $Li[Li_yTi_{2-y}]O_4$. This is probably due to the MIT, resulting in that V_{ave} for $Li[Li_yTi_{2-y}]O_4$ is nearly independent of V_{ave} above 3.6.[4,6]

For $Li[Li_yTi_{2-y}]O_4$, Johnston[4] and Edwards[15] estimated the effective mass for conduction electron (m^*/m_0) and the density of states at the Fermi level $N_0(E_F)$ from A_m. If we ignore the contributions from core diamagnetism and orbital χ, A_m is represented by;

$$A_m = \mu_B^2 (m^*/m_0) N_0(E_F)(1 - m_0^2/3m^{*2}) \tag{5}$$

where the first term corresponds to a Pauli PM contribution and the second term a Landau diamagnetic contribution, m^* is the conduction-electron mass, and m_0 is the free-electron mass. As seen in Table 1, both m^*/m_0 and $N_0(E_F)$ increase with x. Here, when $V_{ave} = 3.5$, $x = 0.83$ in $Li_{1+x}[Li_{1/3}Ti_{5/3}]O_4$. Thus, we compare the data for $Li_{1.83}[Li_{1/3}Ti_{5/3}]O_4$ with that for $Li[Ti_2]O_4$. The magnitude of m^*/m_0 and $N_0(E_F)$ for the former are smaller by 20 % than those for the latter, probably due to a narrow d band character of the electronic structure in $Li[Ti_2]O_4$.

It is interesting to note the relevance between present findings and the reaction mechanism of LTO. To explain the flat operating voltage profile of LTO, Wagemaker et al[26,27] proposed a kinetically induced two-phase region consisting of $Li[Li_{1/3}Ti_{5/3}]O_4$ and $Li_2[Li_{1/3}Ti_{5/3}]O_4$ domains is produced in the LTO compounds with $0 < x < 1$. They also reported that

such region is stable below 100 K, but is unstable at room-T, resulting in the relaxation to a homogeneous solid solution phase of $Li_{1+x}[Li_{1/3}Ti_{5/3}]O_4$.[26,27] Recently grain boundaries between such domains are observed by STEM analyses even at room-T[28,29] However, *in situ* neutron diffraction measurements[30] and ^{7}Li-NMR measurements on chemically Li-inserted LTO[31] indicated the presence of the solid solution phase $Li_{1+x}[Li_{1/3}Ti_{5/3}]O_4$. The existence of T_{m1} in the Li-inserted samples (Fig. 5) supports the two-phase model, whereas the linear dependence of C_m (or A_m) with x [Figs. 6(a) and 6(c)] can be explained by both models. Thus, it is currently difficult to distinguish between $(1-x)Li[Li_{1/3}Ti_{5/3}]O_4 + xLi_2[Li_{1/3}Ti_{5/3}]O_4$ and $Li_{1+x}[Li_{1/3}Ti_{5/3}]O_4$ from the χ data. This difficulty would come from the fact that due to the "zero-strain" character,[2] the local structural environment of the TiO_6 octahedra is nearly unchanged by the occupation of the Li^+ ions at the 8a or 16c site. For instance, even for the $x = 0.94$ compound, the change in the bond length between Ti and O atoms is negligibly small, while the change in bond angles between the O-Ti-O atoms is less than ∼3 degrees compared with the initial state.[20] Therfore, the Li^+ ions at the 16d site rather than those at 8a or 16c site significantly affect the magnetism of LTO, because such Li^+ ions produces a strong perturbation of the itinerant electrons formed by neighboring Ti^{3+} ions.[6]

Finally, we wish to compare the present results with the prediction from first principles calculations. In contrast to $LiTi_2O_4$, first principles calculations on $Li_{1+x}[Li_{1/3}Ti_{5/3}]O_4$ are limited,[25,28,32] because it is difficult to achieve the stoichiometry of LTO and to keep the number of atoms as small as possible. Ouyang et al[25] reported a metallic character of Ti^{3+} ions in $Li_2[Li_{1/3}Ti_{5/3}]O_4$, whereas Lu et al[28] suggested that electrons are fully localized around the Ti^{3+} ions. The present χ measurements demonstrated a more complex nature; i.e., ∼57 % of the d electrons are localized in the $x = 0.95$ sample. Although we have clarified the change in the electronic structure with x, we need to measure specific heat and transport properties for the samples with $x > 0$. in order for further

understanding electronic properties in detail.

5 Conclusions

Magnetic susceptibility (χ) measurements were performed for the $Li_{1+x}[Li_{1/3}Ti_{5/3}]O_4$ (LTO) samples with $x = 0$, 0.50, 0.83, and 0.95, to elucidate the variation of magnetism with x. The samples were prepared by an electrochemical Li insertion reaction. The LTO sample with $x = 0$ exhibited two magnetic anomalies at $T_{m1}(= 63$ K) and $T_{m2}(= 21$ K), although Ti ions in $x = 0$ were believed in a non-magnetic d^0 (4+) state. The raw material, TiO_2 anatase, and Li_2TiO_3 also exhibited similar magnetic anomalies at around 70 and 20 K, whereas TiO_2 ruitle showed no magnetic anomaly as low as 5 K. Thus, T_{m1} and T_{m2} in LTO are considered to be caused by not magnetic impurities but by an intrinsic feature, probably due to either slight compositional deviation from stoichiometry or dislocations such as a Magnéli phase. T_{m1} remained in the χ vs temperature (T) curves for the $x > 0$ samples, suggesting that the region of such non-stoichometry or dislocations does not participate in the electrochemical reaction in LTO.

A Curie-Weiss behavior was evolved with x, in particular below ~ 60 K. This is consistent with the fact that the amount of Ti^{3+} with $S = 1/2$ increases with the Li insertion into the LTO lattice. However, the effective magnetic moment (μ_{eff}) of Ti ions in the $x = 0.95$ sample was estimated to be $0.60(1)$ μ_B, which is ~ 36 % of the full magnetic moment per one Ti ion. In other words, ~ 57 % of the d^1 electrons were localized in all the d^1 electrons in the $x = 0.95$ sample. This indicates an itinerant character of Li-inserted LTO samples, as in the case for $LiTi_2O_4$. Superconductivity was not observed down to 5 K for the $x = 0.83$ and 0.95 samples, although the average valence of Ti ions for the $x = 0.83$ sample is the same to that for superconducting $Li[Ti_2]O_4$.

6 Acknowledgements

References

1 K. M. Colbow, J. R. Dahn and R. R. Haering, *J. Power Sources*, 1989, **26**, 397.

2 T. Ohzuku, A. Ueda and N. Yamamoto, *J. Electrochem. Soc.*, 1995, **142**, 1431.

3 D. C. Johnston, H. Prakash, W. H. Zachariasen and R. Viswanathan, *Mater. Res. Bull.*, 1973, **8**, 777.

4 D. C. Johnston, *J. Low Temp. Phys.*, 1976, **25**, 145.

5 L. J. de Jongh, *Physica C*, 1988, **152**, 171 and references cited therein.

6 M. R. Harrison, P. P. Edwards and J. B. Goodenough, *Philos. Mag.*, 1985, **52**, 679.

7 O. Durmeyer, J. P. Kappler, A. Derory, M. Drillon and J. J. Capponi, *Solid State Commun.*, 1990, **74**, 621.

8 J. Akimoto, Y. Gotoh, K. Kawaguchi and Y. Oosawa, *J. Solid State Chem.*, 1992, **96**, 446.

9 M. Watanabe, K. Kaneda, H. Takeda and N. Tsuda, *J. Phys. Soc. Jpn.*, 1984, **53**, 2437.

10 J. M. Heintz, M. Drillon, R. Kuentzler, Y. Dossmann, J. P. Kappler, O. Durmeyer and F. Gautier, *Z. Phys. B*, 1989, **76**, 303.

11 C. P. Sun, J.-Y. Lin, S. Mollah, P. L. Ho, H. D. Yang, F. C. Hsu, Y. C. Liao and M. K. Wu, *Phys. Rev. B: Condens. Matter Mater. Phys.*, 2004, **70**, 054519.

12 L. Tang, P. Y. Zou, L. Shan, A. F. Dong, G. C. Che and H. H. Wen, *Phys. Rev. B: Condens. Matter Mater. Phys.*, 2006, **73**, 184521.

13 D. P. Tunstall, J. R. M. Todd, S. Arumugam, G. Dai, M. Dalton and P. P. Edwards, *Phys. Rev. B: Condens. Matter Mater. Phys.*, 1994, **50**, 16541.

14 M. R. Harrison, P. P. Edwards and J. B. Goodenough, *J. Solid State Chem.*, 1984, **54**, 136.

15 P. P. Edwards, R. G. Egdell, I. Fragala, J. B. Goodenough, M. R. Harrison, A. F. Orchard and E. G. Scott, *J. Solid State Chem.*, 1984, **54**, 127.

16 M. V. Koudriachova, *Phys. Chem. Chem. Phys.*, 2008, **10**, 5094.

17 S. Hamada, M. Kato, T. Noji and Y. Koike, *Physica C*, 2010, **470**, S766.

18 L. Aldon, P. Kubiak, M. Womes, J. C. Jumas, J. Oliver-Fourcade, J. L. Tirado, J. I. Corredor and C. Pérez Vicente, *Chem. Mater.*, 2004, **16**, 5721.

19 K. Mukai, J. Sugiyama, Y. Ikedo, Y. Aoki, D. Andreica and A. Amato, *J. Phys. Chem. C*, 2010, **114**, 8626.

20 K. Mukai, Y. Kato and H. Nakano, *J. Phys. Chem. C*, 2014, **118**, 2992.

21 K. Mukai and Y. Kato, *J. Phys. Chem. C*, 2015, **119**, 10273.

22 K. Mukai and J. Sugiyama, *Solid State Commun.*, 2010, **150**, 906.

23 L. K. Keys and L. N. Mulays, *Phys. Rev.*, 1967, **154**, 453.

24 Y. Le Page and M. Marezio, *J. Solid State Chem.*, 1984, **53**, 13.

25 C. Y. Ouyang, Z. Y. Zhong and M. S. Lei, *Electrochem. Commun.*, 2007, **9**, 1107.

26 M. Wagemaker, D. R. Simon, E. M. Kelder, J. Schoonman, C. Ringpfeil, U. Haake, D. Lützenkirchen-Hecht, R. Frahm and F. M. Mulder, *Adv. Mater.*, 2006, **18**, 3169.

27 M. Wagemaker, E. R. H. van Eck, A. P. M. Kentgens and F. M. Mulder. *J. Phys. Chem. B*, 2009, **113**, 224.

28 X. Lu, L. Zhao, X. He, R. Xiao, L. Gu, Y.-S,. Hu, H. Li, Z. Wang, X. Duan, L. Chen, J. Maier and Y. Ikuhara, *Adv. Mater.*, 2012, **24**, 3233.

29 M. Kitta, T. Akita, S. Tanaka, M. Kohyama, *J. Power Sources*, 2014, **257**, 120.

30 W. K. Pang, V. K. Peterson, N. Sharma, J.-J. Shiu and S.-H. Wu *Chem. Mater.*, 2014, **26**, 2318.

31 W. Schmidt, P. Bottke, M. Sternad, P. Gollob, V. Hennige and M. Wilkening *Chem. Mater.*, 2015, **27**, 1740.

32 B. Ziebarth, M. Klinsmann, T. Eckl and C. Elsässer, *Phys. Rev. B: Condens. Matter Mater. Phys.*, 2014, **89**, 174301.